# dc conductivity of two-temperature warm dense gold

A. Ng,[1,*] P. Sterne,[2] S. Hansen,[3] V. Recoules,[4] Z. Chen,[5] Y. Y. Tsui,[5] and B. Wilson[2]

[1]*Department of Physics and Astronomy, University of British Columbia, Vancouver, British Columbia, Canada V6T 1Z1*

[2]*Lawrence Livermore National Laboratory, Livermore, California 94550, USA*

[3]*Sandia National Laboratories, Albuquerque, New Mexico 87123, USA*

[4]*CEA, DAM, DIF, 91297 Arpajon Cedex, France*

[5]*Department of Electrical and Computer Engineering, University of Alberta, Edmonton, Alberta, Canada T6G 1H9*

(Received 5 June 2015; published 30 September 2016)

Using recently obtained ac conductivity data we have derived dc conductivity together with free electron density and electron momentum relaxation time in two-temperature warm dense gold with energy density up to 4.1 MJ/kg ($0.8 \times 10^{11}$ J/m$^3$). The derivation is based on a Drude interpretation of the dielectric function that takes into account contributions of intraband and interband transitions as well as atomic polarizability. The results provide valuable benchmarks for assessing the extended Ziman formula for electrical resistivity and an accompanying average atom model.

DOI: 10.1103/PhysRevE.94.033213

dc conductivity, or its inverse, electrical resistivity, is of interest as it contains information on free electron density, ionic structure factor, and electron-ion interaction potential. It may also serve as a surrogate for assessing thermal conductivity via the Wiedemann-Franz law. This is noteworthy. Thermal conductivity is a critical property governing dynamic changes in warm dense matter that are pertinent to experiments and applications involving high-intensity laser-matter interaction. Yet, measurements of thermal conductivity in such states are lacking.

Direct measurements of electrical resistivity in equilibrium warm dense matter near solid densities have been obtained from capillary discharges [1,2], capillary-confined exploding wires [3,4], water-confined exploding wires [5–7], exploding wire z-pinch [8], and high-pressure vessel-confined exploding foils [9–13]. Alternatively, electrical resistivity of similar states has been derived from the self-reflectivity of a 400-fs, 308-nm laser used to heat a 40-nm-thick Al film on glass substrate [14], the reflectivity at 527 nm of tamped laser-heated Al [15], and the reflectivity at 532 nm of polystyrene compressed by laser-driven shock waves [16].

With the availability of femtosecond laser pump-probe techniques to study isochoric heated solids [17], recent interest has turned to nonequilibrium warm dense matter where the electron temperature greatly exceeds the ion temperature. Since the electron-ion energy relaxation time is expected to be 10–100 ps, direct measurements of dc conductivity is not possible. The first attempt to determine dc conductivity of such states was reported by Widmann *et al*. [18]. In their experiment, a 30-nm-thick free-standing Au foil was heated by a 150-fs, 400-nm laser pulse to energy density $<20$ MJ/kg. The reflectivity and transmissivity of the heated sample were measured using a 150-fs, 800-nm laser probe with different delays. The results revealed a quasisteady, isochoric phase with nearly constant reflectivity and transmissivity lasting from $\sim$20 ps for excitation energy density of 0.4 MJ/kg to $\sim$2 ps at 20 MJ/kg. The measured reflectivity and transmissivity were used as input to the Helmholtz equations for electromagnetic wave propagation in a uniform dielectric slab. The solutions yielded the real and imaginary parts of the ac conductivity, $\sigma_r$ and $\sigma_i$. With the top of the $5d$ band of Au at $\sim$2 eV below the Fermi level, interband contribution to ac conductivity at a frequency of 1.55 eV was considered negligible. The measured ac conductivity was assumed to be described by the Drude equations from which the corresponding dc conductivity, free electron density, and electron collision time were derived. Although the results could not be checked against calculations, there was an apparent anomaly that the free electron density remained below the atomic density of Au even for excitation energy density up to 2 MJ/kg [18]. This called into question the neglect of interband contributions to ac conductivity. The need to derive dc conductivity correctly from ac conductivity has become even more pressing with the availability of new data [19].

In this article we present a derivation of dc conductivity from ac conductivity that includes contributions of free electrons, interband transition, and atomic polarizability. Applying this to the results obtained by Chen *et al*. [19], we have eliminated the free electron density anomaly noted above. More importantly, we obtain new results of dc conductivity, free electron density, and electron collision time for assessing theoretical models on two-temperature warm dense Au.

In the experiment of Chen *et al*. [19], a free-standing 30-nm-thick Au foil was heated with a 45-fs (FWHM), 400-nm pump pulse. The ac conductivity of the heated foil was determined from simultaneous measurements of reflectivity and transmissivity using a frequency-chirped probe laser pulse at 800 nm. Here, we focus on the initial state at $\sim$540 fs after the peak of the heating pulse when the heated electrons are thermalized based on the observed thermalization time of $\sim$500–800 fs in fs-laser heated gold at absorbed fluences up to 0.3 mJ/cm$^2$ [20,21]. For this state, we assume that only the electrons are heated while the ions remain at 300 K. This is supported by the good agreement in the measured real part of ac conductivity with theoretical predictions [19].

The ac conductivity in Ref. [19] is first converted into real and imaginary parts of dielectric function

*nga@physics.ubc.ca

 

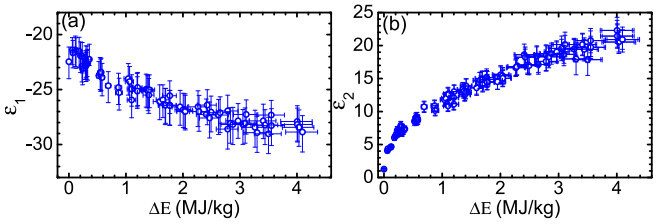


FIG. 1. (a) $\varepsilon_1(\omega)$ and (b) $\varepsilon_2(\omega)$ of nonequilibrium warm dense Au derived from the ac conductivity data of Chen *et al*. [19].

(Fig. 1) for the application of the Drude equations [22]:

$$\varepsilon_1(\omega) = \varepsilon_p + \varepsilon_1^f(\omega) + \varepsilon_1^{ib}(\omega), \tag{1a}$$

$$\varepsilon_2(\omega) = \varepsilon_2^f(\omega) + \varepsilon_2^{ib}(\omega). \tag{1b}$$

Here, $\varepsilon_p = 4\pi n_a \alpha_a$, where $n_a$ is the number of atoms per unit volume and $\alpha_a$ is the atomic polarizability. The ground-state atomic polarizability of Au is $5.8 \times 10^{-24}\text{cm}^3$ [23], attributed to unpublished calculations using the method of Zangwill and Soven [24]. This value is adopted here in the absence of experimental value. The terms due to free electrons are

$$\varepsilon_1^f(\omega) = 1 - \frac{\omega_p^2 \tau^2}{1 + (\omega\tau)^2}, \tag{2a}$$

$$\varepsilon_2^f(\omega) = \frac{\omega_p^2 \tau}{\omega(1 + \omega^2\tau^2)}, \tag{2b}$$

where $\tau$ is the electron collision time, $\omega_p = [4\pi n_e e^2/m^*]^{1/2}$ is the electron plasma frequency, $n_e$ is the free electron density, and $m^*$ is the effective mass of the electrons. Here, $m^*$ is taken to be unity in atomic units at ambient conditions since it has been found to be 0.94–1.06 [22,25–29]. For interband contributions, $\varepsilon_1^{ib}(\omega)$ is derived from $\varepsilon_2^{ib}(\omega)$ using the Kramers-Kronig relation,

$$\varepsilon_1^{ib}(\omega) = \frac{2}{\pi} \int_{\omega_0}^{\infty} \frac{\omega' \varepsilon_2^{ib}(\omega')}{(\omega')^2 - \omega^2} d\omega', \tag{3}$$

where $\omega_0$ is the frequency for the onset of interband transitions.

To evaluate the Kramers-Kronig integral for Au at normal conditions, we first compile $\varepsilon_2(\omega)$ over 0.6–500 eV using the experimental data from Johnson and Christy [30], Canfield *et al*. [31], Hagemann *et al*. [32], Nilsson [33], and Zombeck *et al*. [34] [Fig. 2(a)]. The onset of $5d$-$6s$ transitions appears at 1.9 eV. Accordingly, $\varepsilon_2(\omega)$ below 1.9 eV represents contributions from free electrons only. Its best fit to the Drude equation (2 b) for $\varepsilon_2^f(\omega)$ is illustrated in Fig. 2(a), together with an extrapolation (red-dashed line) to higher frequencies. This yields $\omega_p = 1.36 \pm 0.02 \times 10^{16}$ rad/s and $\tau = (9.4 \pm 1.4)$ fs, leading to $n_e = (5.84 \pm 0.14) \times 10^{22}\,\text{cm}^{-3}$ that is in good agreement with one free electron per atom and dc conductivity $\sigma_0 = [\omega_p^2 \tau/(4\pi)] = (1.4 \pm 0.25) \times 10^{17}\,\text{s}^{-1}$ or resistivity of $(6.5 \pm 0.4)\,\mu\Omega$ cm that is consistent with $5.9 \pm 0.5\ \mu\Omega$ cm obtained from a standard four-point resistivity measurement

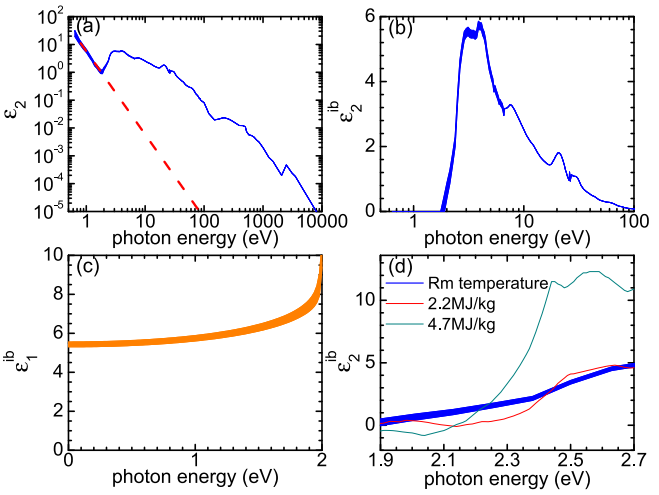


FIG. 2. (a) $\varepsilon_2(\omega)$, (b) $\varepsilon_2^{ib}(\omega)$, (c) Kramers-Kronig values of $\varepsilon_1^{ib}(\omega)$ for Au at normal conditions, and (d) the imaginary part of the dielectric function observed by Ping *et al*. [36].

[35] of the Au foils used. These values of $\varepsilon_2^f(\omega)$ are then used in Eq. (1b) to yield $\varepsilon_2^{ib}(\omega)$ in Fig. 2(b). Figure 2(c) shows the corresponding Kramers-Kronig value of $\varepsilon_1^{ib}(\omega)$. The increasing effect of the $5d$-$6s$ transition as photon energy approaches 2 eV is evident. At 1.55 eV, this yields $\varepsilon_1^{ib}(\omega) = 6.38 \pm 0.19$.

Returning to the experimental data in Fig. 1, we first consider the dielectric function at 1.55 eV under normal conditions. From the measured value of $\varepsilon(\omega) = (-22.4 \pm 1.8) + i(1.26 \pm 0.10)$, our interpretation using Eqs. (1) and (2) together with $\varepsilon_1^{ib}(\omega) = 6.38 \pm 0.19$ yields $\omega_p = (1.38 \pm 0.06) \times 10^{16}$ rad/s and $\tau = (11.9 \pm 2.0)$ fs. These lead to $\sigma_0 = [\omega_p^2 \tau/(4\pi)] = (1.84 \pm 0.45) \times 10^{17}\,\text{s}^{-1}$ and a corresponding electrical resistivity of $(5.25 \pm 1.25)\,\mu\Omega$ cm that is consistent with $6.5\,\mu\Omega$ cm noted above. To obtain $n_e$ from $\omega_p$, $m^*$ is again taken to be unity in atomic units. This yields $(5.99 \pm 0.45) \times 10^{22}\,\text{cm}^{-3}$, in agreement with the atomic density of Au.

Before applying our interpretation to warm dense gold, we need to consider possible changes of $\varepsilon_1^{ib}(\omega)$ with excitation energy density. As yet, there is no validated calculation of $\varepsilon(\omega)$ of two-temperature warm dense gold. The only available guidance is the dielectric function observed by Ping *et al*. [36]. From their measured $\varepsilon_2(\omega)$ (Fig. 3(b) in Ref. [36]) we have extracted $\varepsilon_2^{ib}(\omega)$ at excitation energy density of 2.2 and 4.7 MJ/kg as presented in Fig. 2(d). The values of $\varepsilon_1^{ib}(\omega)$ in the spectral range of 1.5–2.7 eV are found to be ~6.2 at 2.2 MJ/kg and ~8.1 at 4.7 MJ/kg, using the Kramers-Kronig relation. Compared with its ambient value of 6.38, $\varepsilon_1^{ib}(\omega)$ increases by 1.7 at 4.7 MJ/kg. This is relatively minor since $\varepsilon_1(\omega)$ has also changed from (−22.4) at ambient conditions to (−28.5) even at 4.1 MJ/kg [Fig. 1(a)]. Accordingly we have neglected the dependence of $\varepsilon_2^{ib}(\omega)$ on temperature in this work, keeping its value constant at $6.38 \pm 0.19$. By applying Eqs. (1) and (2) to the data in Fig. 1, we derive $\omega_p$ and $\tau$ to yield $n_e$ and $\sigma_0$. The results for $n_e$, $\tau$, and $\sigma_0$ are presented in Fig. 3.

A long-standing method for calculating electrical resistivity is the extended Ziman formulation [37] that leads

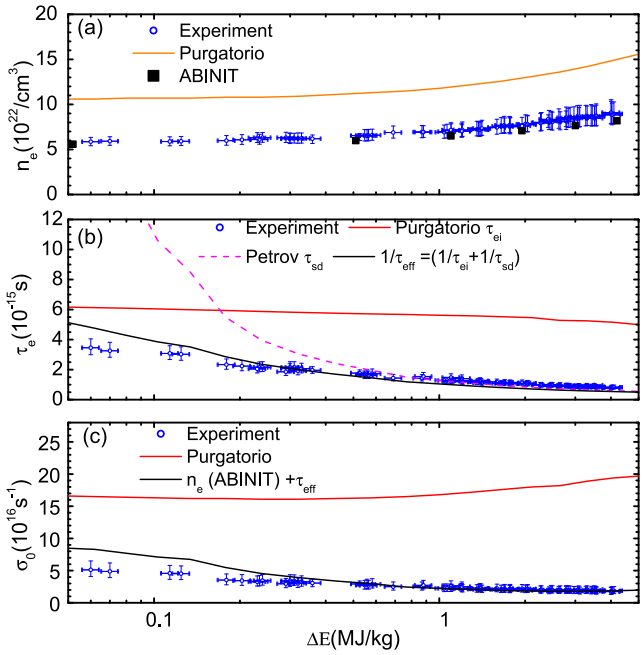


FIG. 3. (a) Free electron density, (b) electron relaxation time, and (c) dc conductivity derived from measured dielectric function of nonequilibrium warm dense Au.

to [38]

$$\eta = \frac{1}{3\pi\alpha}\left(\frac{\Omega_0}{Z_i}\right)^2 \frac{1}{\Omega_0} \times \int_0^\infty d\epsilon \frac{d}{d\epsilon} f_{\beta\mu}(\epsilon) \int_0^{2p} dq q^3 S(q)\sigma_\epsilon(q), \quad (4)$$

where $\eta$ is the resistivity, $\alpha$ is the fine structure constant, $\Omega_0$ is the atomic volume, $Z_i$ is the ion charge, $f_{\beta\mu}(\epsilon)$ is the Fermi-Dirac distribution function, $\beta$ is the inverse temperature, $\mu$ is the chemical potential, $S(q)$ is the ion-ion structure factor, and $\sigma_\epsilon(q)$ is the electron-ion cross section for momentum transfer for electron energy $\varepsilon$. This can also be expressed in a Drude form of $\eta = (4\pi/\omega_p^2)\tau$ where $\tau$ is the electron-ion collision time. The input parameters to Eq. (4) are $Z_i$, $\sigma_\epsilon(q)$, and $S(q)$.

To apply the Ziman formulation we follow the work of Hansen *et al.* [39] that is based on an implementation of a DFT approach with an average atom model in the PURGATORIO code [40]. Specifically, the wave functions of bound and free electrons are obtained as solutions of the Dirac equations that incorporate a Kohn-Sham exchange potential [41], a correlation potential due to Perdew and Zunger [42], and a Coulomb potential for the ion core. $Z_i$ is evaluated from the ideal density of state $X^{\text{ideal}}(\varepsilon)$ that excludes quasibound or resonant states,

$$Z_i = \int_0^\infty f(\varepsilon,\mu) X^{\text{ideal}}(\varepsilon) d\varepsilon. \quad (5)$$

Furthermore, the cross section for momentum exchange $\sigma_\epsilon(q)$ is expressed as

$$\sigma_\epsilon(q) = \int_0^{2p} q^3 \left(\frac{d\sigma(p,\theta)}{d\theta}\right) S(q) dq, \quad (6)$$

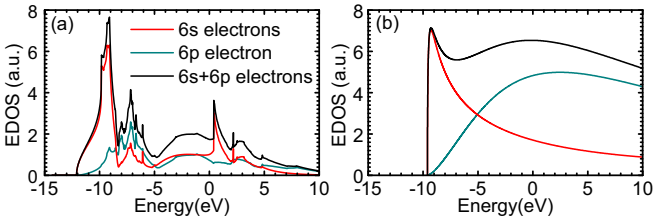


FIG. 4. Electron density of states of solid-density Au calculated with (a) ABINIT at an electron temperature of 3 eV and (b) PURGATORIO at an electron temperature of 3 eV.

where the differential cross section $\frac{d\sigma(p,\theta)}{d\theta}$ is obtained from the scattering cross sections in the average ion potential. The relativistic dispersion relation $p^2 = \varepsilon(2+\varepsilon\alpha^2)$ is assumed and the integration is performed over the momentum transfer vector $q^2 = 2p^2(1-\cos\theta)$. For the isochoric heated state of interest, the ion structure factor $S(q)$ of solid gold is used in our calculation.

This approach is designed to generate reasonable equation-of-state data and transport properties for any ion over a very wide range of conditions. Clear, it has several drawbacks: The ion-sphere approach excludes correlations that are important at low ion temperatures [43,44] and the transport integral given in Eq. (4) draws on cross sections not derived from a consistent potential (as in Ref. [45]). Nonetheless, conductivities calculated with this approach capture general qualitative trends observed in the sparse collection of experimental data in the regime of interest here.

Turning our attention first to $Z_i$, we find that Eq. (5) yields $n_e = Z_i n_i$ of $1.07 \times 10^{23}\text{cm}^{-3}$ at ambient conditions. This is ~1.8 times the atomic density of gold. The calculated $n_e$ continues to exceed the experimental values by a similar factor throughout our observation [Fig. 3(a)]. Interestingly, both the theoretical results and our presented results show a similar scaling with excitation energy density. This prompted an alternative approach to derive $n_e$, using the electron structure calculated from the density functional theory–molecular dynamics (DFT-MD) code ABINIT [46]. Here, the Kohn-Sham equations for electrons are solved using a Kohn-Sham exchange potential, a correlation potential due to Perdew and Wang [47], and a projector augmented wave (PAW) data set that has been extensively tested [48]. This yields the $s$-projected, $p$-projected, and $d$-projected electron density of states. An example is shown in Fig. 4(a) for an electron temperature of 3 eV, corresponding to an excitation energy density of 4.5 MJ/kg. The electron temperature is calculated from the excitation energy density using the electron specific heat $C_e(T_e)$ given by the derivative of the total electron energy density $U$ with respect to the electron temperature $T_e$ at constant volume $V$ [49],

$$C_e = \left(\frac{\partial U}{\partial T_e}\right)_V. \quad (7)$$

This expression contains all thermal effects within DFT, including the temperature dependence of the electron density of states. The free electron density is evaluated from the occupied $6s$ and $6p$ states. This yields $n_e = 5.49 \times 10^{22}\,\text{cm}^{-3}$ at ambient conditions, close to the atomic density of gold. It also

yields $n_e$ that is in good agreement with our values as illustrated in Fig. 3(a). The difference in $n_e$ calculated from ABINIT and PURGATORIO can readily be traced to differences in the electron density of states (DOS) derived from the two codes. From Figs. 4(a) and 4(b) for $T_e = 3$ eV, it is evident that PURGATORIO yields higher values of DOS for $6s$ and $6p$ electrons, so that even excluding the $5d$ resonance states, as prescribed by Eq. (5), leads to an overestimate of the free electron density. This behavior persists down to zero K. This difference is due to a feature in PURGATORIO that requires local charge neutrality within the atomic sphere. In the case of gold, the $5d$ electrons extend beyond the radius of the equilibrium-volume atomic sphere, resulting in only 9.2 $5d$ electrons within the sphere. The shortfall is compensated for by increasing the chemical potential, which adds an additional 0.8 $s$-$p$ electrons and accounts for the observed factor of 1.8 increase in $Z_i$. This is clearly an artifact resulting from the charge-neutrality ansatz used in PURGATORIO. This ansatz is commonly used in many atom-in-jellium codes. The present result indicates that care must be applied to ensure that the results of interest are not an unphysical consequence of this ansatz. Concerns with this ansatz have been noted before [50]. Here, we have not tried to remedy this problem—we simply note that it is present, and its effect is to increase the effective value of $Z_i$ over the temperature and density range for which the $5d$ states are occupied. The error introduced will reduce with increasing temperature. The quantitative value for the conductivity is altered, but the qualitative variations with temperature are less affected, as shown by the similar variations between PURGATORIO and ABINIT in Fig. 3(a).

Next we compare $\tau$ and $\sigma_0$ derived from the Ziman formula to our values. As shown in Figures 3(b) and 3(c), further discrepancies are evident. In particular, the increase in the calculated values of $\sigma_0$ with excitation energy density above $\sim$0.2 MJ/kg is a striking contrast to the observed scaling. As shown in Eq. (4), our implementation of the Ziman formula takes into account only the change in momentum of the conduction electrons via electron-ion scattering. This is adequate for describing Au at low electron temperature with a filled $5d$ band. However, for the warm dense states of interest vacancies are created in the $5d$ band. Scattering by the remaining bound $5d$ electrons lead to the change in momentum of the $6s$ and $6p$ electrons. To account for its effect on electrical conductivity, we construct an effective collision frequency $\nu_{eff} = (\nu_{ei} + \nu_{sd})$ where $\nu_{ei} = 1/\tau_{ei}$ is the electron-ion collision frequency, $\tau_{ei}$ is the electron-ion collision time obtained from the Ziman calculation in PURGATORIO, and $\nu_{sd}$ is the frequency of collisions between $6s$ and $6p$ electrons with $5d$ electrons that is given in a total electron collision frequency $\nu_{se} = (\nu_{sd} + \nu_{ss})$ calculated by Petrov *et al.* [51], where $\nu_{ss}$ is the frequency of collisions among the $6s$ and $6p$ electrons that conserve their total momentum. This total frequency was recently used by Fourment *et al.* in the interpretation of experimental results [52]. Here, we extract $\nu_{sd}$ from $\nu_{se}$ using $\nu_{ss}$ calculated from the best fit given in Ref. [51], which interpolates between dynamic screening of degenerate relativistic electrons and static screening of Coulomb interaction at higher temperatures. As illustrated in Fig. 3(b), the resulting effective collision time $\tau_{\text{eff}} = 1/\nu_{\text{eff}}$ shows significantly better agreement with experimental data above 0.5 MJ/kg. At lower energy density, the discrepancy may result from the polycrystalline structure of the Au foils while the calculations describe a single crystal. It can also be seen in Fig. 3(c) that the value of $\sigma_0$ calculated using $n_e$ from ABINIT together with $\tau_{\text{eff}}$ yields similar improvement, in agreement with our values. This is encouraging but some caveats should be noted. The electron collision frequencies are derived from different models and the effect of overestimating $n_e$ on $\nu_{ss}$ and $\nu_{ei}$ is not known. Change of momentum may also result from electron-electron scattering via Umkalpp processes [53] but the corresponding collision frequency in warm dense gold is not known.

It may be noted that using a Drude fit of $\sigma_r$ calculated from the Kubo-Greenwood formula to derive $\sigma_0$ is not practical with ABINIT. Convergence of result cannot be reached as the energy resolution of the eigenstates is limited by the number of atoms in the simulation cell [54]. The alternative approach of calculating $\sigma_0$ directly from the Kubo-Greenwood formula is beyond the scope of this work.

In conclusion, we have obtained a new set of free electron density, electron collision time, and dc conductivity values using a Drude interpretation of the measured ac conductivity of two-temperature warm dense gold. These are compared with calculations based on an average atom model and the Ziman formula for electrical resistivity. The average atom model appears to overestimate the electron density by a factor of $\sim$1.8 in comparison with experiment and DFT-MD calculation. This has been shown to be due to the charge-neutrality ansatz in the PURGATORIO model. Greater discrepancies are found between our calculated and interpreted electron collision time and dc conductivity. The calculation of electron collision time can be improved by taking into account the scattering of $6s$ and $6p$ electrons with $5d$ electrons. Improvement in the calculation of dc conductivity requires the additional correction of electron density using results of density functional theory implemented in solid-state physics codes.

We wish to thank M. W. C. Dharma-wardana for many valuable discussions and research funding from the Natural Sciences and Engineering Research Council of Canada.

[1] R. L. Shepherd, D. R. Kania, and L. A. Jones, Phys. Rev. Lett. **61**, 1278 (1988).
[2] J. F. Benage, Jr., W. R. Shanahan, E. G. Sherwood, L. A. Jones, and R. J. Trainor, Phys. Rev. E **49**, 4391 (1994).
[3] A. W. DeSilva and H. J. Kunze, Phys. Rev. E **49**, 4448 (1994).
[4] J. Kirsch and H. J. Kunze, Phys. Rev. E **58**, 6557 (1998).
[5] A. W. DeSilva and J. D. Katsouros, Phys. Rev. E **57**, 5945 (1998).
[6] T. Sasaki, Y. Yano, M. Nakajima, T. Kawamura, and K. Horioka, Laser Part. Beams **24**, 371 (2006).
[7] T. Sasaki, M. Nakajima, T. Kawamura, and K. Horioka, Phys. Plasmas **17**, 084501 (2010).

[8] J. F. Benage, W. R. Shanahan, and M. S. Murillo, Phys. Rev. Lett. **83**, 2953 (1999).

[9] V. Recoules, P. Renaudin, J. Clerouin, P. Noiret, and G. Zerah, Phys. Rev. E **66**, 056412 (2002).

[10] J. Clerouin, P. Renaudin, Y. Laudernet, P. Noiret, and M. P. Desjarlais, Phys. Rev. B **71**, 064203 (2005).

[11] P. Renaudin, V. Recoules, P. Noiret, and J. Clerouin, Phys. Rev. E **73**, 056403 (2006).

[12] J. Clerouin, C. Starrett, G. Faussurier, Ch. Blanchard, P. Noiret, and P. Renaudin, Phys. Rev. E **82**, 046402 (2010).

[13] J. Clerouin, C. Starrett, P. Noiret, P. Renaudin, C. Blancard, and G. Faussurier, Contrib. Plasma Phys. **52**, 17 (2012).

[14] H. M. Milchberg, R. R. Freeman, S. C. Davey, and R. M. More, Phys. Rev. Lett. **61**, 2364 (1988).

[15] A. N. Mostovych and Y. Chan, Phys. Rev. Lett. **79**, 5094 (1997).

[16] M. Koenig, F. Philippe, A. Benuzzi-Mounaix, D. Batani, M. Tomasini, E. Henry, and T. Hall, Phys. Plasmas **10**, 3026 (2003).

[17] A. Forsman, A. Ng, G. Chiu, and R. M. More, Phys. Rev. E **58**, R1248 (1998).

[18] K. Widmann, T. Ao, M. E. Foord, D. F. Price, A. D. Ellis, P. T. Springer, and A. Ng, Phys. Rev. Lett. **92**, 125002 (2004).

[19] Z. Chen, B. Holst, S. E. Kirkwood, V. Sametoglu, M. Reid, Y. Y. Tsui, V. Recoules, and A. Ng, Phys. Rev. Lett. **110**, 135001 (2013).

[20] W. S. Fann, R. Storz, H. W. K. Tom, and J. Bokor, Phys. Rev. Lett. **68**, 2834 (1992); Phys. Rev. B **46**, 13592 (1992).

[21] C. K. Sun, F. Vallee, L. Acioli, E. P. Ippen, and J. G. Fujimoto, Phys. Rev. B **48**, 12365 (1993).

[22] M. L. Theye, Phys. Rev. B **2**, 3060 (1970).

[23] T. M. Miller, in *CRC Handbook of Chemistry and Physics*, 94th ed. (CRC Press, Boca Baton, FL, 1970).

[24] A. Zangwill and P. Soven, Phys. Rev. A **21**, 1561 (1980).

[25] J. N. Hodgson, J. Phys. Chem. Solids **29**, 2175 (1968).

[26] L. G. Schulz, J. Opt. Soc. Am. **44**, 540 (1954).

[27] B. R. Cooper, H. Ehreneich, and H. R. Philipp, Phys. Rev. **138**, A494 (1965).

[28] G. P. Motulevich and A. A. Shubin, Zh. Eksp. Teor. Fiz. **47**, 840 (1964) [Sov. Phys. JETP **20**, 560 (1965)].

[29] D. Beaglehole, Proc. Phys. Soc. London **87**, 461 (1966).

[30] P. B. Johnson and R. W. Christy, Phys. Rev. B **6**, 4370 (1972).

[31] L. R. Canfield, G. Hass, and W. R. Hunter, J. Phys. **25**, 124 (1964).

[32] H. J. Hagemann, W. Gudat, and C. Kunz, J. Opt. Soc. Am. **65**, 742 (1965).

[33] P. O. Nilsson, Phys. Kondens. Mater. **11**, 1 (1970).

[34] M. V. Zombeck, G. K. Austin, and D. T. Torgerson, Smithsonian Astrophysical Observatory Report SAO-AXAF-90-003, Cambridge, Massachusetts, 1980 (unpublished).

[35] L. J. van der Pauw, Philips Tech. Rev. **20**, 220 (1958).

[36] Y. Ping, D. Hanson, I. Koslow, T. Ogitsu, D. Prendergast, E. Schwegler, G. Collins, and A. Ng, Phys. Rev. Lett. **96**, 255003 (2006).

[37] R. Evans, B. L. Gyroffy, N. Szabo, and J. M. Ziman, in *The Properties of Liquid Metals*, edited by S. T. Takeuchi (Wiley, New York, 1973).

[38] G. A. Rinker, Phys. Rev. B **31**, 4207 (1985).

[39] S. B. Hansen, W. A. Isaac, P. A. Sterne, B. G. Wilson, V. Sonnad, and D. A. Young, Lawrence Livermore National Laboratory, Livermore, CA UCRC-PROC-218150, 2006 (unpublished).

[40] B. Wilson, V. Sonnad, P. Sterne, and W. Isaac, J. Quant. Spectrosc. Radiat. Transfer **99**, 658 (2006).

[41] W. Kohn and L. J. Sham, Phys. Rev. **140**, A1133 (1965).

[42] J. P. Perdew and A. Zunger, Phys. Rev. B **23**, 5048 (1981).

[43] F. Perrot and M. W. C. Dharma-Wardana, Phys. Rev. A **36**, 238 (1987).

[44] M. W. C. Dharma-Wardana, Phys. Rev. E **73**, 036401 (2006).

[45] G. Faussurier and C. Blancard, Phys. Rev. E **91**, 013105 (2015).

[46] X. Gonze, B. Amadon, P.-M. Anglade *et al.*, Comput. Phys. Commun. **180**, 2582 (2009).

[47] J. P. Perdew and Y. Wang, Phys. Rev. B **45**, 13244 (1992).

[48] A. Dewaele, M. Torrent, P. Loubeyre, and M. Mezouar, Phys. Rev. B **78**, 104102 (2008).

[49] B. Holst, V. Recoules, S. Mazevet, M. Torrent, A. Ng, Z. Chen, S. E. Kirkwood, V. Sametoglu, M. Reid, and Y. Y. Tsui, Phys. Rev. B **90**, 035121 (2014).

[50] T. Blenski, R. Piron, C. Caizergues, and B. Cichocki, High Energ. Dens. Phys. **9**, 687 (2013).

[51] Yu.V. Petrov, N. A. Inogamov, and K. P. Migdal, JETP Lett. **97**, 20 (2013).

[52] C. Fourment, F. Deneuville, D. Descamps, F. Dorchies, S. Petit, O. Peyrusse, B. Holst, and V. Recoules, Phys. Rev. B **89**, 161110(R) (2014).

[53] A. A. Abrikosov, *Fundamentals of the Theory of Metals* (North-Holland, Amsterdam, 1988), Chap. 4.

[54] M. Pozzo, M. P. Desjarlais, and D. Alfè, Phys. Rev. B **84**, 054203 (2011).